Steel and Composite Structures, *Vol. 16, No. 1 (2014) 99-116*
DOI: http://dx.doi.org/10.12989/scs.2014.16.1.099

Experimental study on circular concrete filled steel tubes with and without shear connectors

K. Chithira [a] and K. Baskar [*]

Department of Civil Engineering, National Institute of Technology, Tiruchirappalli 620 015, Tamilnadu, India

(*Received March 18, 2011, Revised September 10, 2013, Accepted September 23, 2013*)

Abstract. This paper deals with a study on ultimate strength behaviour of eccentrically loaded CFT columns with and without shear connectors. Thirty specimens are subjected to experimental investigation under eccentric loading condition. P-M curves are generated for all the test specimens and critical eccentricities are evaluated. Three different D/t ratios such as 21, 25 and 29 and L/D ratios varying from 5 to 20 are considered as experimental parameters. Six specimens of bare steel tubes as reference specimens, twelve specimens of CFT columns without shear connectors and twelve specimens of CFT columns with shear connectors, in total thirty specimens are tested. The P-M values at the ultimate failure load of experimental study are found to be well agreed with the results of the proposed P-M interaction model. The load-deflection and load-strain behaviour of the experimental column specimens are presented. The behaviour of the CFT columns with and without shear connectors is compared. Experimental results indicate that the percentage increase in load carrying capacity of CFT columns with shear connectors compared to the ordinary CFT columns is found to be insignificant with a value ranging from 6% to 13%. However, the ductility factor of columns with shear connectors exhibit higher values than that of the CFT columns without shear connectors. This paper presents the proposed P-M interaction model and experimental results under varying parameters such as D/t and L/D ratios.

Keywords: CFT; shear connector; P-M interaction; ductility

1. Introduction

Application of composite tubular columns is becoming highly popular due to their better structural performance compared to that of hollow steel tubes and reinforced concrete columns. In particular, circular tubular columns have an advantage over other sections when used as compression members. For a given cross sectional area, they have a large uniform flexural stiffness in all directions. In addition, filling the bare steel tube with concrete increases the ultimate strength of the member without significant increase in cost, as well as workability and fire resistance. Research on CFT column has been ongoing worldwide for many decades, with significant contributions having been made.

Shakir-Khalil (1993a, b) carried out a series of push-out tests on CFT columns with different

∗Corresponding author, Associate Professor, E-mail: drkbaskar@yahoo.co.in
[a] Ph.D. Student, E-mail: chitrasuresh@ymail.com

http://www.techno-press.org/?journal=scs&subpage=8 ISSN: 1229-9367 (Print), 1598-6233 (Online)

types of shear connectors and concluded that the wall thickness of the steel tube and the amount of shear connectors used in the CFT columns greatly influenced the shear resistance.

O'Shea and Bridge (2000) developed several design methods that can be used to conservatively estimate the strength of circular thin-walled concrete filled steel tubes under different loading conditions such as (i) Axial loading on the steel only; (ii) Axial loading on the concrete only; and (iii) Axial and eccentrical loading on both concrete and steel.

Lakshmi and Shanmugam (2002) predicted the behaviour of concrete filled steel tubes (Square, Rectangular and Circular) by using a semi-analytical method. Moment-curvature-thrust relationships were generated for column cross sections by an iterative process.

Shanmugam *et al*. (2002) proposed a method using an effective width principle to predict the behaviour and load carrying capacity of thin-walled steel tubes with concrete in-fill.

Zhang *et al*. (2003) presented test results of eight high strength concrete-filled square steel tubes subjected to eccentric compression.

Chen and Hikosaka (2003) tested eighteen specimens of short concrete filled steel tube columns under eccentric compression. The interpretation of the experimental results indicated that the effect of eccentricity ratio was most remarkable on the behaviour and ultimate load carrying capacity of CFST eccentric columns.

Fujimoto *et al*. (2004) investigated the effect of higher material strengths on the flexural behaviour of CFT columns through sixty five test specimens under eccentric loading.

Zeghiche and Chaoui (2005) conducted 27 tests on concrete-filled steel tubular columns. The test parameters were the column slenderness, the load eccentricity covering axially and eccentrically loaded columns with single or double curvature bending and the compressive strength of the concrete core.

Liu (2006) presented an experimental and analytical study of the behaviour of high-strength rectangular concrete-filled steel tubular (CFT) columns subjected to eccentric loading. Favourable ductility performance was observed for all specimens during the tests. An analytical model was developed to predict the behaviour of high-strength rectangular CFT columns subjected to eccentric loading.

Gopal and Manoharan (2006) studied the behaviour of twelve slender steel tubular columns of circular sections filled with both plain and fibre reinforced concrete. The specimens were tested under eccentric compression to investigate the effects of fibre reinforced concrete on the strength and behaviour of slender composite columns. Interpretation of the experimental results indicated that the use of fibre reinforced concrete as infill material has a considerable effect on the strength and behaviour of slender composite columns.

Lu *et al*. (2007) obtained the bending moment–axial force–curvature (M–N–ϕ) relation for eccentrically compressed square CFT by basic analysis of mechanics which have taken into account the effect of residual stress of steel and non-linearity of concrete and steel.

De Nardin and El Debs (2007) dealt with the contribution of headed stud bolt shear connectors and angles to improve the shear resistance of the steel-concrete interface using push-out tests. The test results indicated that the mechanical shear connectors were very efficient to decrease the concrete slip and to increase the maximum load capacity. The angles were more efficient than the stud bolts in increasing the load capacity and reducing the slip at maximum load applied.

Hatzigeorgiou (2008) dealt with the behaviour and capacity of circular concrete-filled tube stub columns under extreme loading conditions. New method had been proposed for the capacity of axial and eccentrically loaded circular CFT columns. The comparisons between numerical, analytical and experimental results demonstrated that the proposed method provided very good

numerical performance for predicting the behaviour of circular CFT columns.

Choi *et al*. (2008) proposed simplified strength equations that can be conveniently used to establish a P-M interaction curve of square concrete filled tubes (CFTs) with concrete strength of up to 100 MPa.

Liang (2008) presented a nonlinear finite element analysis method for determining the axial load–moment strength interaction diagrams for short concrete-filled steel tubular (CFST) beam–columns under axial load and biaxial bending.

Xiao *et al*. (2012) presented an experimental study on the shear capacity of circular concrete filled steel tube (CCFT) specimens with and without axial compression force and shear capacity, ductility, and damage modes of CCFTs were investigated and compared. The test results indicated that the several factors including section size, material properties, shear span ratio, axial compression ratio, and confinement index affected the shear capacity of CCFTs.

Huang *et al*. (2012) studied the structural performance of concrete filled circular steel tube columns subjected to four concentric loading schemes through the experimental investigation. The generalized prediction method has been developed and evaluated the ultimate load capacity of CFST columns subjected to various loading conditions.

Patel *et al*. (2012) presented a multiscale numerical method for simulating the interaction local and global buckling behaviour of high strength thin walled rectangular CFST slender beam-columns under eccentric loading. The numerical model were utilized to investigate the effects of concrete compressive strength, depth to thickness ratio, loading eccentricity ratio and column slenderness ratio on the performance indices.

Many of above literatures are dealt with CFT columns. However, the majority of these experiments have been on columns using normal and high strength concrete, subjected to concentric or eccentric loading and only a few researches were on concentrically loaded CFT columns with shear connectors. This paper presents the details of an experimental investigation on the behaviour of eccentrically loaded CFT column (both short and long) with and without shear connectors.

In view of understanding the behaviour of such column sections, an experimental investigation is carried out in this study through thirty column specimens. The pin ended specimens are tested under eccentrical load. Three different D/t ratios such as 21, 25 and 29 with slenderness ratios varying from 5 to 20 are considered as test parameters. The results are discussed in detail in this paper.

2. Details of the test specimens

A total of thirty column specimens under three different groups are tested under eccentric load condition. Group-1 consists of specimens having diameter 87.6 mm with wall thickness of 3.04 mm (i.e., D/t ratio of 28.82, rounded to 29). Group-2 consists of specimens having diameter 75.3 with wall thickness of 3.05 (i.e., D/t ratio of 24.69, rounded to 25) and the Group-3 consists of specimens having diameter 60.4 mm with wall thickness of 2.86 mm (i.e., D/t ratio of 21.12, rounded to 21). Rounded values are used in the following discussions. In each group, two hollow steel tubes (H), four Concrete Filled Tubes (CFT) and four Concrete Filled Tubes with Shear Connectors (CFTC) with various L/D ratios (5, 8, 11 and 20) are investigated. The properties of each specimen are given in Table 1. In total, 6 hollow steel tubes, 12 Concrete Filled Steel Tubes and 12 Concrete Filled Steel Tubes with shear connectors are considered in the present study.

2.1 Specimen notations

Details of test specimens are shown in Table 1. The specimen ID is designated by an alphanumeric system. The alphabets 'H' refer to Hollow tubes, CFT tubes refer to Concrete Filled Tubes and CFTC refers to Concrete Filled Steel Tubes with Shear Connectors. The first following number refers to D/t Group and second number refers to actual L/D ratio.

3. Material properties

3.1 Steel

Tensile strength tests are carried out on tube materials through standard coupons. The coupon specimens conforming to ASTM A370 (2003) are prepared for each tube material which is shown in Fig. 1 and are subjected to test. Typical stress-strain curve of bare steel tube is shown in Fig. 2. The Yield strength and Ultimate strength are obtained as 283 MPa and 420 MPa respectively. The modulus of elasticity is calculated as 1.98×10^5 N/mm^2.

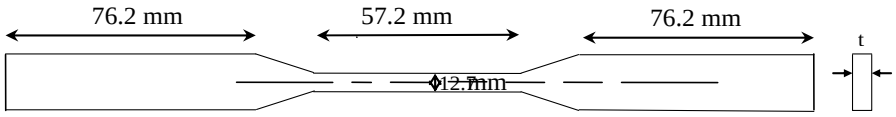

Fig. 1 Dimensions of tensile coupon test specimen. (Ref: ASTM A370)

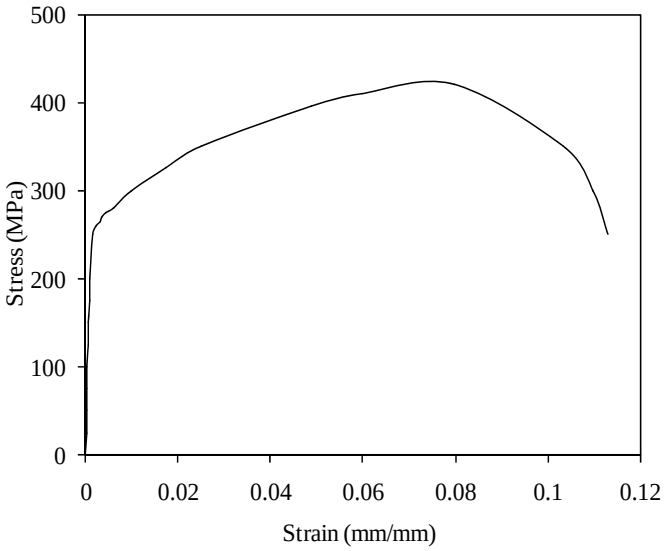

Fig. 2 Stress- strain curve of steel

3.2 Concrete

Ingredient materials required for concrete infill are collected from the locally available source and are tested for its physical properties. A Mix Design is carried out based on the Indian Standard (IS 10262-1982) to achieve M30 grade concrete and the mix proportion is as follows.

Water	Cement	Fine aggregate	Coarse aggregate
0.48	1	1.337	2.372

In order to characterize the mechanical behaviour of infill concrete, twelve numbers of 150 × 150 × 150 mm cubes and eight numbers of 150 × 300 mm cylinders are prepared and tested. The mean value of compressive strength at 7th day is 35.43 MPa and at 28th day is 43.58 MPa. The modulus of elasticity is calculated as 33 GPa. The test results are conforming to the acceptance criteria as per IS 456 (2000).

4. Cross sectional analysis

4.1 Development of P-M interaction curve

Chen and Atsuta (1972, 1974) have developed the interaction equation for solid circular sections. Based on the techniques used for development of P-M interaction model for solid circular sections are extended to the case of Concrete Filled Steel Tube cross sections. The proposed equations for axial force and bending moment about X-axis for the circular Concrete Filled Steel columns (CFT) by rigid plastic approach is given by

Total force =

$$\begin{aligned} P = {} & \sigma_y\{r_o^2(\phi_o - 0.5\sin 2\phi_o) - r_i^2(\phi_i - 0.5\sin 2\phi_i)\} + f_{ck}\{r_i^2(\phi_i - 0.5\sin 2\phi_i)\} \\ & - \sigma_y\{\pi(r_0^2 - r_i^2) - [r_o^2(\phi_o - 0.5\sin 2\phi_o) - r_i^2(\phi_i - 0.5\sin 2\phi_i)]\} \end{aligned} \tag{1}$$

The moment about horizontal axis is given by

$$\begin{aligned} M_x = {} & \sigma_y[(r_o^3/2)\cos\theta_o(\sin\phi_o - 1/3\sin 3\phi_o) - (r_i^3/2)\cos\theta_i(\sin\phi_i - 1/3\sin 3\phi_i)] \\ & + f_{ck}[(r_i^3/2)\cos\theta_i(\sin\phi_i - 1/3\sin 3\phi_i)] + 0.5(r_0^2 - r_i^2)(r_0 + r_i)\sigma_y - A_3 y\sigma_y \end{aligned} \tag{2}$$

A_3 and y values are given in Eqs. (3)-(4).

$$A_3 = 0.5\pi(r_0^2 - r_i^2) - A_{sc} \tag{3}$$

$$\begin{aligned} y = {} & \{0.5(r_0^2 - r_i^2)(r_0 + r_i) - [(r_o^3/2)\cos\theta_o(\sin\phi_o - 1/3\sin 3\phi_o) \\ & - (r_i^3/2)\cos\theta_i(\sin\phi_i - 1/3\sin 3\phi_o)]\} / (0.5\pi(r_0^2 - r_i^2) - A_{sc}) \end{aligned} \tag{4}$$

Eqs. (1)-(2) are the required P and M equations for developing the interaction relation. Eccentricity ‘e’ is incremented by small values and the corresponding P & M values are obtained. The above iterative process is carried out for the condition NA lying within the section. The P-M

interaction curve has been generated by using C Programming and MATLAB.

The above proposed P-M interaction model is validated, with the previously published experimental results of O'Shea and Bridge (2000) and Zeghiche and Chaoui (2005).

5. Selection of the eccentricity 'e' from the P-M interaction curve

In the present study, the P-M curves as shown in Fig. 3 are generated for the three groups of test specimens. From the P-M curves, the critical eccentricities have been taken for the eccentric

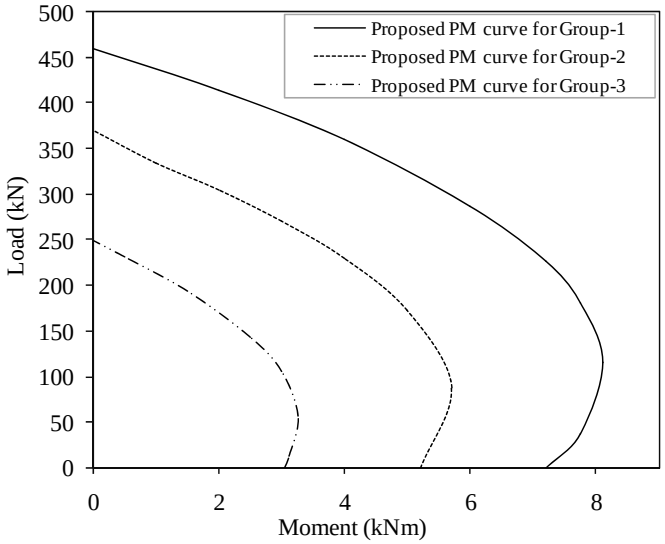

Fig. 3 P-M Interaction curve for the test specimens

Fig. 4 Typical view of the experimental setup

load application. The critical eccentricities are calculated as the ratio between the maximum moments to the corresponding loads which are given in Table 1. The experimental setup as shown in Fig. 4 is designed to withstand the maximum eccentric load.

Table 1 Detail of test specimens

Sl. No	Specimen ID	Outside diameter	Wall thickness	Length of specimen	D/t ratio	L/D ratio	Eccentricity of experimental load
		D (mm)	*t* (mm)	*L* (mm)			*e* (mm)
1	CFT.1.5	88	3.04	440.00	29	5	70
2	CFT.1.8	88	3.04	701.00	29	8	70
3	CFT.1.11	88	3.04	966.00	29	11	70
4	CFT.1.20	88	3.04	1760.00	29	20	70
5	H.1.8	88	3.04	705.00	29	8	70
6	CFTC.1.5	88	3.04	440.00	29	5	70
7	CFTC.1.8	88	3.04	700.50	29	8	70
8	CFTC.1.11	88	3.04	964.00	29	11	70
9	CFTC.1.20	88	3.04	1760.00	29	20	70
10	H.1.20	88	3.04	1756.00	29	20	70
11	CFT.2.5	75	3.05	376.00	25	5	65
12	CFT.2.8	75	3.05	599.00	25	8	65
13	CFT.2.11	75	3.05	824.00	25	11	65
14	CFT.2.20	75	3.05	1505.00	25	20	65
15	H.2.11	75	3.05	820.00	25	11	65
16	CFTC.2.5	75	3.05	374.00	25	5	65
17	CFTC.2.8	75	3.05	601.00	25	8	65
18	CFTC.2.11	75	3.05	825.00	25	11	65
19	CFTC.2.20	75	3.05	1505.00	25	20	65
20	H.2.20	75	3.05	1506.00	25	20	65
21	CFT.3.5	60	2.86	303.00	21	5	58
22	CFT.3.8	60	2.86	484.00	21	8	58
23	CFT.3.11	60	2.86	665.00	21	11	58
24	CFT.3.20	60	2.86	1191.00	21	20	58
25	H.3.11	60	2.86	661.00	21	11	58
26	CFTC.3.5	60	2.86	301.00	21	5	58
27	CFTC.3.8	60	2.86	477.00	21	8	58
28	CFTC.3.11	60	2.86	661.00	21	11	58
29	CFTC.3.20	60	2.86	1191.00	21	20	58
30	H.3.20	60	2.86	1191.00	21	20	58

6. Test setup and procedure

All the experiments are carried out through a newly erected 100 Ton capacity loading frame as shown in Fig. 4. Eccentric load is applied through a 200 Ton capacity hydraulic jack by an electrically operated hydraulic pump. Details of experimental setup, test specimens and testing procedure are explained in detail in the following sections.

6.1 Loading frame

A 100 Ton capacity loading frame as shown in Fig. 4 has been designed and erected in the structural engineering lab. It has two numbers of 1060 mm × 615 mm × 120 mm plates and four self supporting columns of diameter 100 mm. Twelve hexagonal nuts are provided over the 100 mm Ø column sections for vertical height adjustment of the top plate. The entire experimental setup has been mounted in between the thick plates. Experimental setup is described in the following section.

6.2 Experimental setup

Fig. 4 shows the test set up of an eccentrically loaded CFT column. The columns are hinged at the ends and the load is applied through designed eccentricity. The eccentricities are equal at both ends and columns are subjected to single curvature bending. A tight fit circular steel collar is provided at the two ends of specimens to transfer the axial force and bending moment without any slip. This collar is replaced for each group upon the completion. The whole setup has been mounted on the load cell having capacity of 500 kN. A difference in capacity of loading frame, hydraulic pump/jack and load cell may be noticed in this discussion. 50% efficiency is expected in hydraulic jack and pump and therefore, a 200 ton capacity jack/pump is used in the 100 ton frame. The expected failure load of the test specimens is less than 50 ton and therefore, a 500 kN load cell is used.

6.3 Preparation of the test specimens

All the steel specimens have been cut for the required L/D ratios, and the edges are flattened well for uniform loading. High strength bolts Grade-4.6 as per IS 1364-Part 1(2002) of length 50 mm has been bent as shown in Fig. 5 and used as a shear connector. The bent portion of the bolt shear connector is inserted inside and welded to the outer steel surface as shown in Fig. 5. The connector's spacing is chosen similar to the specifications given for steel concrete composite beams in Euro Code 4 (2004). The bent lengths for each group of specimen and the spacing between the shear connectors are given in Table 2. During the preparation of the test specimens, the specimens are kept in vertical position and the casting is done in layers with proper compaction to avoid air voids in concrete.

6.4 Instrumentation

All the specimens are instrumented with two electrical strain gauges to record the extreme fibre strains on the diagonally opposite faces, both in tension and compression side of the steel tubes at the mid-height of the columns. Two Linearly Varying Displacement Transducers (LVDT) as shown in Fig. 4 are used to measure the axial deformation and are placed diametrically opposite to

each other. A 50 Ton strain gauge based load cell is used to measure the applied load. Load is applied till the failure of specimen. All the data from the load cell, strain gauges and LVDTs are scanned at frequency of one Hertz and the data are stored using 16 channel data logger. Also, experiments are conducted to evaluate the efficiency of shear connectors in CFT columns to improve the overall structural behaviour of such columns and are explained in the following sections.

7. Results and discussions

7.1 Verification of the proposed P-M interaction with experimental results

The P-M interaction curves have been plotted for the test specimens of Group-1, Group-2 and Group-3 columns and are shown in Figs. 6-8 using the proposed P-M Eqs. (1)-(2). The critical eccentricities have been calculated from the proposed P-M interaction curves as discussed in the sec. 5. The above specimens are tested under the calculated critical eccentric loading conditions and the test results are illustrated in Figs. 6-8. It is noted that the P-M values at the ultimate failure load of experimental study are found to be agreed with the results of the proposed P-M interaction model.

7.2 Load versus deflection behaviour

The non linear load-axial deformations for all the thirty tested columns are drawn and are shown in Figs. 9 to 20. The load-deformation behaviour for CFT columns having L/D ratios 5 and 8 with and without shear connectors for Group-1 columns has been presented in Figs. 9-10. The ultimate load of Group-1 columns having slenderness ratio 5 is 120.23 kN and it is reduced to

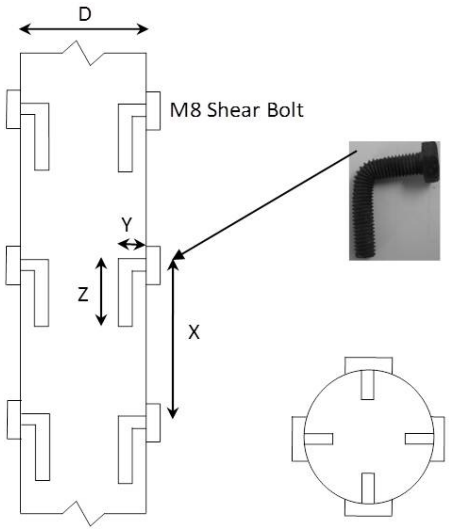

Fig. 5 Typical view of shear connectors

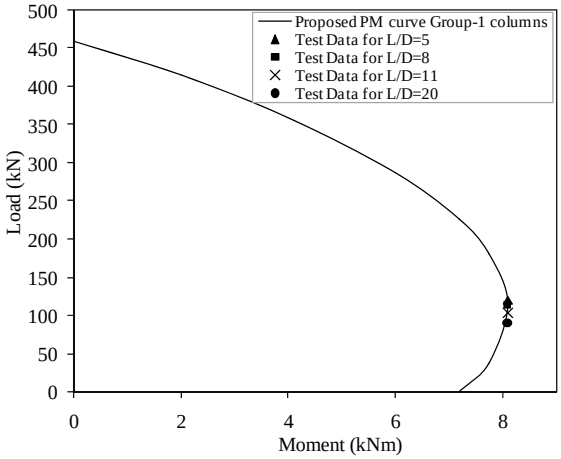

Fig. 6 P-M Interaction curve for Group-1 columns

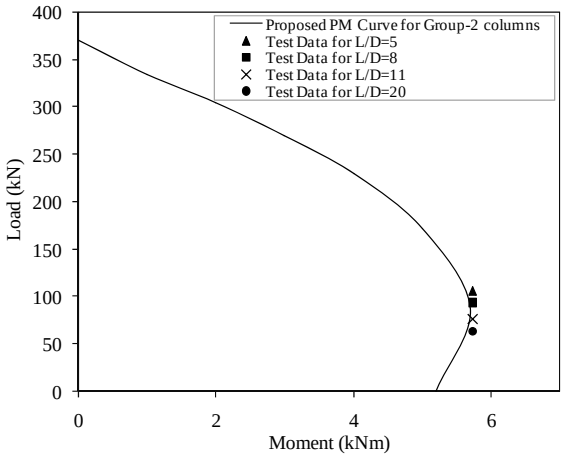

Fig. 7 P-M Interaction curve for Group-2 columns

Table 2 Details of the shear connectors

Sl. No	Type of shear connector	Yield strength (N/mm^2)	Ult. tensile strength (N/mm^2)	% of elongation	Specimen D (mm)	Spacing between shear connector X (mm)	Horizontal bent length Y (mm)	Vertical bent length Z (mm)
1					88	90	20	30
2	Grade 4.6	240	400	22	75	85	20	30
3					60	87	10	40

90.67 kN when the slenderness ratio is increased to 20 and the same that of the CFTC column is 138.01 kN and 99.92 kN. The percentage increases in load carrying capacity of such column varies from 12.88% to 9.26% when the column is strengthened by shear connectors and are give in Table 3. The comparison clearly indicates that the ultimate load carrying capacity decreases while increasing the slenderness ratio from 5 to 20.

The Load deformation behaviour of Group-2 columns is shown in Figs. 13-16. For CFTC columns, the percentage increase in load carrying capacity varying from 11.52% to 5.95% while increasing the slenderness ratio from 5 to 20, when compared to CFT columns.

The non linear Load-Axial deformation behaviour of Group-3 columns are shown in Figs. 17-20. The load carrying capacity is increased by 10.71% to 12.11% in CFTC columns for L/D ratio varying from 5 to 20. This is due to strengthening of CFT columns by shear connectors.

From the comparison of load deformation behaviour of all the CFT columns, it is noted that the short columns showed a linear behaviour up to yield load and after showed a non linear behaviour. A sudden drop in the load carrying capacity is found with larger deformation after ultimate load. But in the CFTC columns, after reaching the ultimate load, ultimate load is maintained for increasing axial deformation.

It is observed that the slender column behaves in a different manner. Both CFT and CFTC columns undergo large deformation after reaching the ultimate load. In comparison with the reference column, the ultimate strength of the composite columns both with and without shear

connectors is approximately 21% to 30% and 14% to 26% higher.

Comparison of load versus strain (ratio of change in length to original length due to buckling) for Group-2 column having L/D ratio 8 is given in Fig. 21. From the figure, it can be noted that extreme fibre compressive strains ranging from 0.002 to 0.003 are reached. The figure shows that, after reaching the ultimate load the strain level is increased. Larger strain value is noted in the post failure stage. Same behaviour is noted for other columns also. It can be seen that CFTC columns behaved in a stiff manner than the CFT columns. Even though, there is no significant increase in load carrying capacity of the eccentrically loaded CFTC columns, such columns offer more ductility than the CFT columns and are explained in the following section.

7.3 Ductility behaviour

The ductility factor for CFT column with shear connector is calculated as ratio between the deflections at yielding of extreme fibre to the deflections at failure point corresponding to the ultimate load of CFT column (D_u/D_y) and is tabulated in Table 3. Figs. 9-10 show the axial deformation versus load curve for the CFT columns having L/D ratios 5 and 8 with without shear connectors. From the graph, ductility factor is obtained as 5.17 for the CFTC.1.5 and 3.07 for CFTC.1.8.

It clearly shows that in the case of CFT columns with shear connector, after the yield point the load keeps on increasing upto the ultimate load and then it reduces slowly upto failure point. But in the CFT column, there is no significant load increment between yield point and failure point at the ultimate load level.

Table 3 Results of CFT columns with and without shear connectors

Sl.No	Specimen detail	Ultimate load in hollow tube (kN)	Ultimate load in CFT (kN)	Ultimate load in CFTC (kN)	% increase on ultimate load	Deflection at yield point D_y (mm)	Deflection at failure point D_u (mm)	Ductility factor in CFTC corresponding to the ultimate load of CFT
		H	CFT	CFTC				
1	1.5		120.23	138.01	12.88	4.50	23.25	5.17
2	1.8	93.82	113.19	125.45	9.77	6.50	20.00	3.07
3	1.11		102.89	112.71	8.71	8.00	22.25	2.81
4	1.20	72.00	90.67	99.92	9.26	10.00	33.00	3.30
5	2.5		106.28	120.13	11.52	8.25	33.25	4.03
6	2.8		92.83	102.26	9.22	8.25	32.00	3.88
7	2.11	64.03	75.95	81.73	7.08	11.00	28.00	2.55
8	2.20	47.74	64.15	68.21	5.95	13.50	32.00	2.37
9	3.50		51.62	57.81	10.71	3.50	22.00	6.28
10	3.80		47.97	53.04	9.55	6.00	23.00	3.83
11	3.11	36.60	41.88	46.00	8.94	5.75	17.25	3.00
12	3.20	32.60	35.33	40.20	12.11	7.00	23.00	3.28

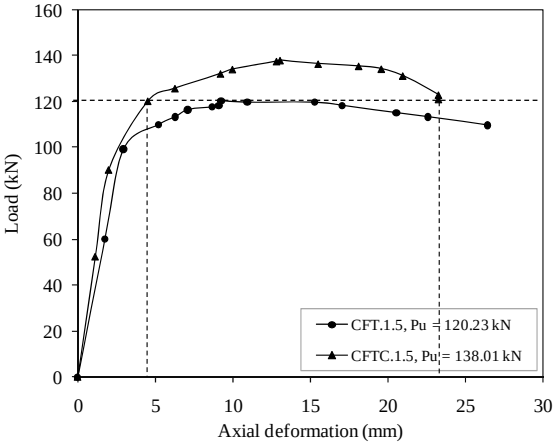

Fig. 9 Comparison of load-deformation behaviour between CFT.1.5 and CFTC.1.5

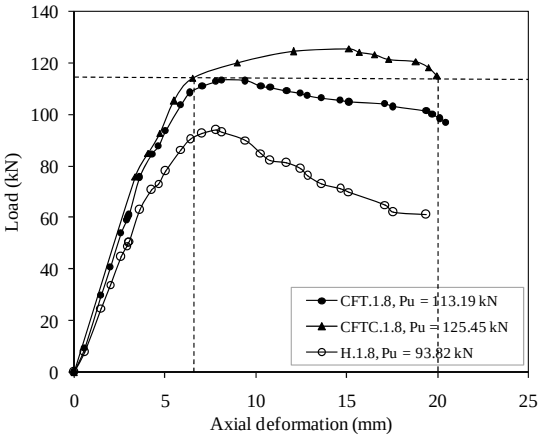

Fig. 10 Comparison of load-deformation behaviour between H.1.8, CFT.1.8 and CFTC.1.8

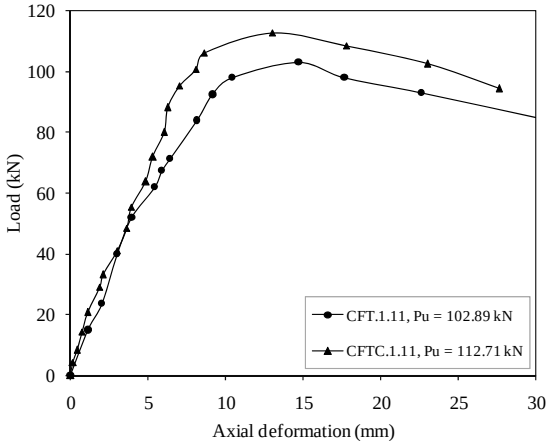

Fig. 11 Comparison of load-deformation behaviour between CFT.1.11 and CFTC.1.11

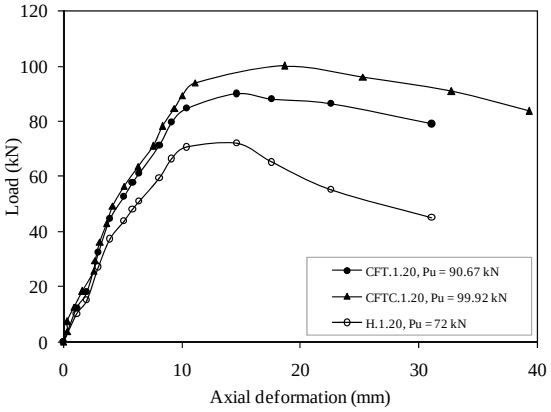

Fig. 12 Comparison of load-deformation behaviour between H.1.20, CFT.1.20 and CFTC.1.20

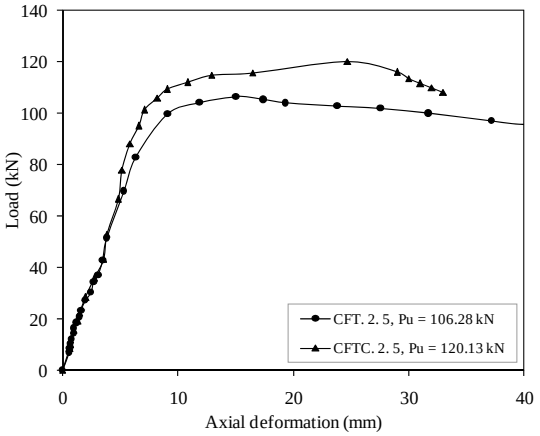

Fig. 13 Comparison of load-deformation behaviour between CFT.2.5 and CFTC.2.5

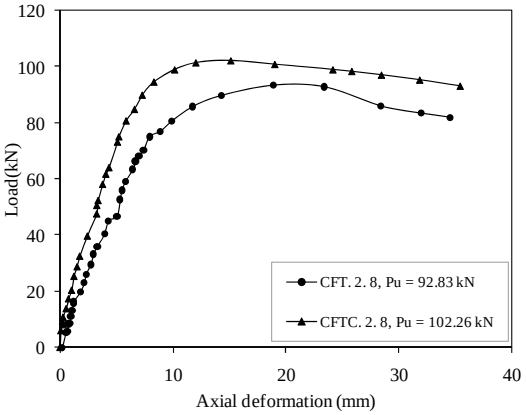

Fig. 14 Comparison of load-deformation behaviour between CFT.2.8 and CFTC.2.8

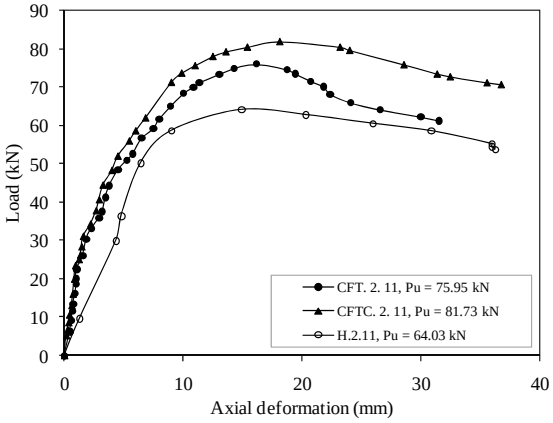

Fig. 15 Comparison of load-deformation behaviour between H.2.11, CFT.2.11 and CFTC.2.11

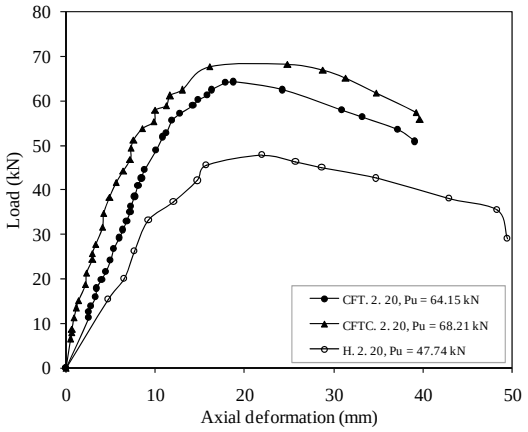

Fig. 16 Comparison of load-deformation behaviour between H.2.20, CFT.2.20 and CFTC.2.20

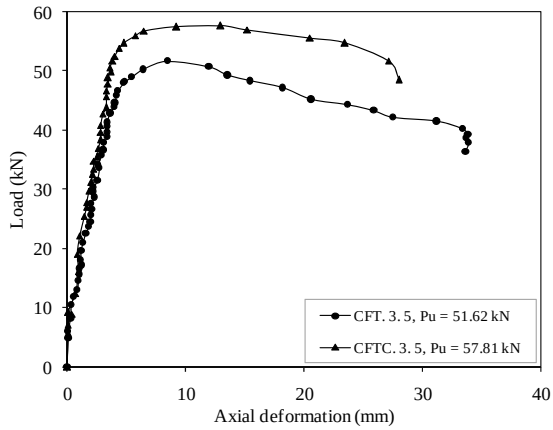

Fig. 17 Comparison of load-deformation behaviour between CFT.3.5 and CFTC.3.5

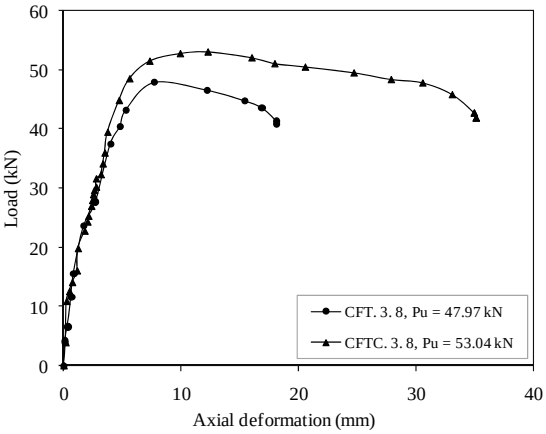

Fig. 18 Comparison of load-deformation behaviour between CFT.3.8 and CFTC.3.8

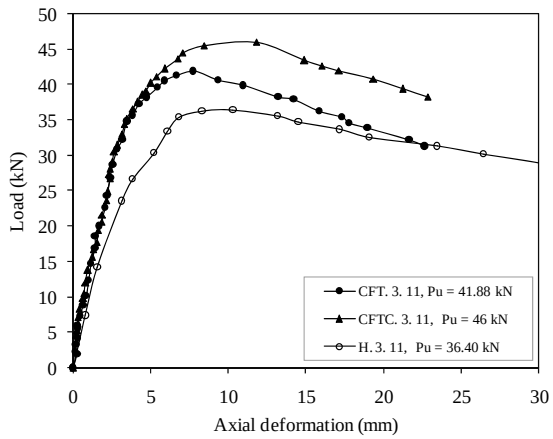

Fig. 19 Comparison of load-deformation behaviour between H.3.11, CFT.3.11 and CFTC.3.11

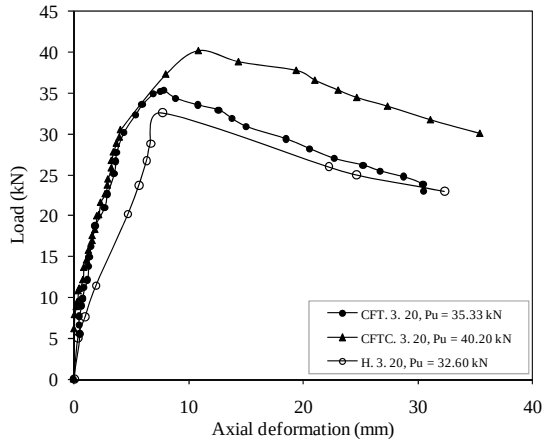

Fig. 20 Comparison of load-deformation behaviour between H.3.20, CFT.3.20 and CFTC.3.20

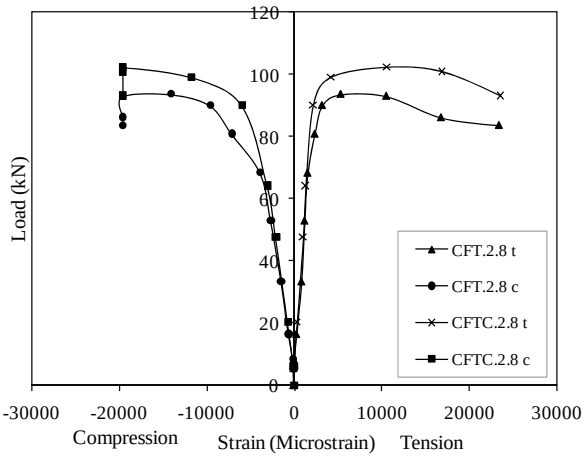

Fig. 21 Comparison of load-strain behaviour between CFT.2.8 and CFTC.2.8

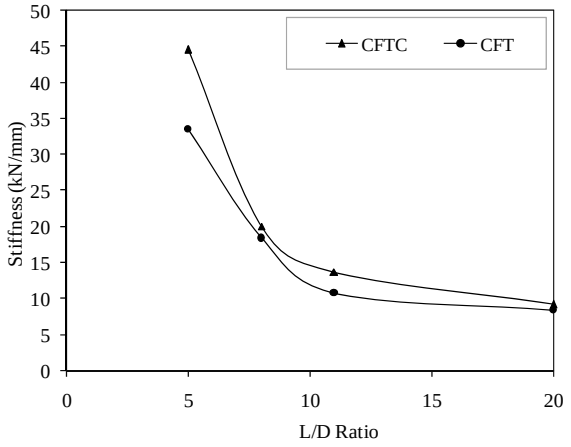

Fig. 22 Stiffness versus L/D ratio for Group-1 columns

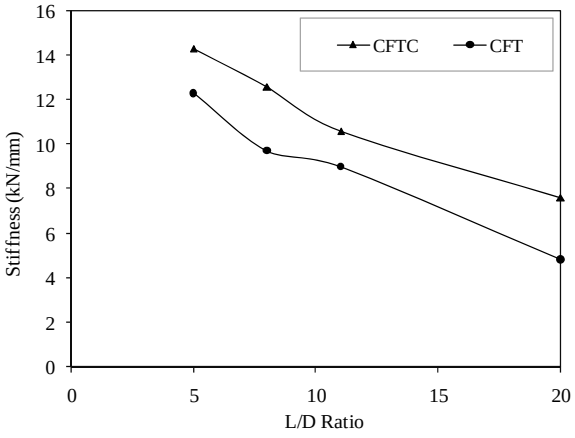

Fig. 23 Stiffness versus L/D ratio for Group-2 columns

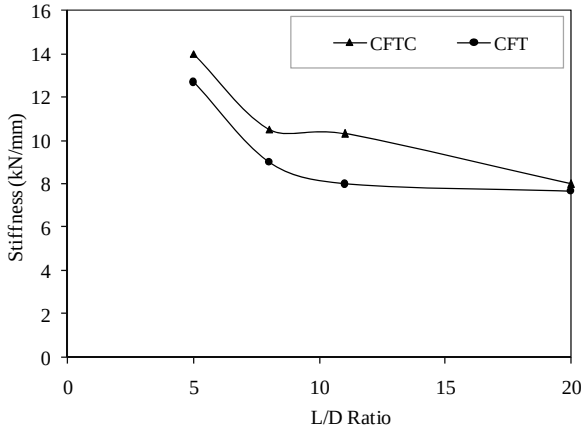

Fig. 24 Stiffness versus L/D ratio for Group-3 columns

By providing the shear connectors, better ductility performance is noted in the CFT columns with shear connectors when compared to the CFT column at the ultimate load point. Hence, structures with CFTC can be used in seismic areas for improved structural behaviour.

7.4 Effect of L/D *ratio on stiffness*

Stiffness is defined as the ability to resist lateral deformation, and stiffness values are calculated as the ratio of the load increment to the corresponding axial deformation and are given in Table 3. The variations in stiffness of all the column specimens are shown in Figs. 22-24. It is observed that the stiffness decreases with an increase in L/D ratio. Also, it shows quite clearly that CFTC columns behaved in a stiff manner than that of CFT columns. In general, the stiffness of the CFT column is much higher than that of empty steel tubes.

7.5 Buckling behaviour

The buckling modes observed during the experiment are reported in Figs. 25(a)-(c). Results are used to study the relation between buckling failure modes and section capacities and are discussed below. It is noticed that the column buckles at the mid height due to concrete crushing and steel yielding in the compression zone.

The load vs. axial deformation behaviour of specimens H.1.8, CFT.1.8 and CFTC.1.8 are shown in Fig. 10. A ultimate load of 93.82 kN is reached for a axial deformation of 7.83 mm in H.1.8 column. The monotonic axial load is given until collapse of the specimen. The column member initially failed in global buckling mode and there after inward local buckling mode of failure at middle. The global and local buckling mode of failure is shown in Fig. 25(a) for the specimen H.1.8.

(a) (b) (c)

Fig. 25 (a) Global and local buckling of H.1.8; (b) Global and local buckling of CFT.1.8; and (c) Global buckling of CFTC.1.8

From the Fig. 25(b), the outward local buckling of 16 mm is occurred at 400 mm from top of the specimen CFT.1.8. The final length of the column measured is 685 mm. It concludes that the infill concrete restrains the inward local buckling in the steel tubes.

The global buckling mode of failure is shown in Fig. 25(c) for the specimen CFTC.1.8. From the figure, it is noted that there is no occurrence of local buckling in the entire length of the specimen. This shows that the shear connector used is found to improve the buckling strength of the column.

8. Conclusions

The results obtained from the tests on CFT with and without shear connectors are presented in this paper.

The P-M interaction curves have been plotted for the test specimens using the proposed P-M equations. The critical eccentricities are calculated from the proposed P-M interaction curves and the specimens are tested under the calculated critical eccentric loading conditions. It is noted that the percentage difference between P-M values at the ultimate failure load of experimental study and proposed P-M interaction model are within 10%.

The use of shear connectors has resulted in considerable improvement in the structural behaviour of composite columns subjected to eccentric loading with respect to ultimate load carrying capacity, stiffness and ductility. From load versus deformation curve, the percentage increase in load carrying capacity is varying from 12.88% to 9.26% for Group-1 CFTC columns, 11.52% to 5.95% for Group-2 CFTC columns and 10.71% to 12.11% for Group-3 columns having L/D ratio varying from 5 to 20, when compared with CFT columns. Also, it shows quite clearly that CFTC columns behaved in a stiff manner than that of CFT columns.

The contribution of the shear connector in CFTC columns has shown better ductility performance than the ordinary CFT columns. Hence, structures with CFTC can be used in seismic areas for improved structural behaviour.

The CFTC columns did not show any signs of local buckling of the shell and the columns are able to sustain more loads before global buckling failure.

Acknowledgments

The research described in this paper was financially supported by National Institute of Technology, Trichy, India.

References

ASTM International (A370, 2003), *Standard Test Methods and Definitions for Mechanical Testing of Steel Products*.

Chen, B.C. and Hiroshi, H. (2003), "Eccentricity ratio effects on the behaviour of eccentrically loaded CFST columns", *Advances in Structures*, Hancock *et al*. (eds), Swets & Zeitlinger, Lisse, ISBN 90.

Chen, W.F. and Atsuta, T. (1972), "Interaction equations for biaxially loaded sections", *J. Struct. Div*., *ASCE*, **98**(5), 1035-1052.

Chen, W.F. and Atsuta, T. (1974), "Interaction curves for steel sections under axial load and biaxial

bending", *Can. Soc. Civil Eng., Eng. J.*, 17, I-VIII.
Choi, Y.H., Kim, K.S. and Choi, S.M. (2008), "Simplified P-M interaction curve for square steel tube filled with high-strength concrete", *Thin-Walled Struct.*, **46**(5), 506-515.
De Nardin, S. and El Debs, A.L.H.C. (2007), "Shear transfer mechanisms in composite columns: an experimental study", *Steel Compos. Struct., Int. J.*, **7**(5), 377-390.
Euro Code 4 (EC 4, 2004) European Committee of Standardisation (draft: Design of composite steel and concrete structures).
Fujimoto, T., Mukai, A., Nishiyama, I. and Sakino, K. (2004), "Behaviour of eccentrically loaded concrete-filled steel tubular columns", *J. Struct. Eng.*, **130**(2), 203-212.
Gopal, S.R. and Manoharan, P.D. (2006), "Experimental behaviour of eccentrically loaded slender circular hollow steel columns in-filled with fibre reinforced concrete", *J. Construct. Steel Res.*, **62**(5), 513-520.
Hatzigeorgiou, G.D. (2008), "Numerical model for the behaviour and capacity of circular CFT columns, Part II: Verification and extension", *Engineering Structures*, **30**(6), 1579-1589.
Huang, F.Y., Yu, X.M. and Chen, B.C. (2012), "The structural performance of axially loaded CFST columns under various loading conditions", *Steel Compos. Struct., Int. J.*, **13**(5), 451-471.
IS 10262 (1982), *Indian Standard Recommended Guidelines for Concrete Mix Design*, Bureau of Indian Standards, New Delhi, India.
IS 456 (2000), *Indian Standard Plain and Reinforced Concrete – Code of Practice*, Bureau of Indian Standards, New Delhi, India.
IS 1364: Part 1 (2002), *Specifications for Hexagon Head Bolts, Screws and Nuts of Product Grades A & B*, Bureau of Indian Standards, New Delhi, India.
Lakshmi, B. and Shanmugam, N.E. (2002), "Nonlinear analysis of in-filled steel-concrete composite columns", *J. Struct. Eng.*, **128**(7), 922-933.
Liang, Q.Q. (2008), "Nonlinear analysis of short concrete-filled steel tubular beam–columns under axial load and biaxial bending", *J. Construct. Steel Res.*, **64**(3), 295-304.
Liu, D.L. (2006), "Behaviour of eccentrically loaded high-strength rectangular concrete-filled steel tubular columns", *J. Construct. Steel Res.*, **62**(8), 839-846.
Lu, F.W., Li, S.P. and Sun, G.J. (2007), "A study on the behaviour of eccentrically compressed square concrete-filled steel tube columns", *J. Construct. Steel Res.*, **63**(7), 941-948.
O'Shea, M.D. and Bridge, R.Q. (2000), "Design of circular thin-walled concrete filled steel tubes", *J. Struct. Eng.*, **126**(11), 1295-1303.
Patel, V.I., Liang, Q.Q. and Hadi, M.N.S. (2012), "Inelastic stability analysis of high strength rectangular concrete-filled steel tubular slender beam-columns", *Interact. Multiscale Mech., Int. J.*, **5**(2), 91-104.
Shakir-Khalil, H. (1993a), "Pushout strengths of concrete-filled steel hollow sections", *The Structural Engineer*, 71(13), 230-233.
Shakir-Khalil, H. (1993b), "Resistance of concrete-filled steel tubes to pushout forces", *Struct. Eng.*, **71**(13), 234-243.
Shanmugam, N.E., Lakshmi, B. and Uy, B. (2002), "An analytical model for thin-walled steel box columns with concrete in-fill", *Eng. Struct.*, **24**(6), 825-838.
Xiao, C.Z., Cai, S.H., Chen, T. and Xu, C.L. (2012), "Experimental study on shear capacity of circular concrete filled steel tubes", *Steel Compos. Struct., Int. J.*, **13**(5), 437-449.
Zeghiche, J. and Chaoui, K. (2005), "An experimental behaviour of concrete-filled steel tubular columns", *J. Construct. Steel Res.*, **61**(1), 53-66.
Zhang, S.M., Guo, L.H. and Tian, H. (2003), "Eccentrically loaded high strength concrete-filled square steel tubes", *Advances in Structures*, Hancock *et al.* (eds), Swets& Zeitlinger, Lisse, ISBN 90.

CC

Nomenclature

A_{sc} (e, r)	Area of steel in compression
CFT	Concrete filled steel tubular columns
CFTC	Concrete filled steel tubular columns with shear connectors
CFST	Concrete-filled steel tubular beam-columns
CA	Centroidal axis
D/t	Diameter to thickness ratio
DF	Ductility factor
E	Young's modulus (N/mm^2)
f_{ck}	Characteristic compressive strength of concrete
f_y	Yield stress
GPa	Giga pascal (kN/mm^2)
IS	Indian standard code of practice
L/D	Length to diameter ratio
LVDT	Linearly varying displacement transducers
MPa	Mega pascal (N/mm^2)
M_x	Total moment about the X-axis
NA	Neutral axis
P	Total force
P–M	Load-moment interaction curve
r	Mean radius
r_i	Inner radius
r_o	Outer radius
ϕ_o	Outer curvature
ϕ_i	Inner curvature
θ_o	Outer angle of twist
θ_i	Inner angle of twist